Molecular Biology of the Cell
Vol. 14, 1418–1432, April 2003

# Extracellular Signal-regulated Kinase Mediates Phosphorylation of Tropomyosin-1 to Promote Cytoskeleton Remodeling in Response to Oxidative Stress: Impact on Membrane Blebbing

**François Houle,* Simon Rousseau,† Nick Morrice,† Mario Luc,* Sébastien Mongrain,* Christopher E. Turner,‡ Sakae Tanaka,§ Pierre Moreau,‖ and Jacques Huot*¶**

*Le Centre de Recherche en Cancérologie de l'Université Laval, L'Hôtel-Dieu de Québec, Québec G1R 2J6, Canada; †Medical Research Council Phosphorylation Unit, School of Life Sciences, University of Dundee, Dundee DD1 5EH, United Kingdom; ‡Department of Cell and Developmental Biology, Upstate Medical University, Syracuse, New York 13210; §Department of Orthopaedic Surgery, Faculty of Medicine, The University of Tokyo, Tokyo 113-0033, Japan; and ‖Faculté de Pharmacie, Université de Montréal, Montréal H3C 3J7, Canada

Submitted April 26, 2002; Revised November 27, 2002; Accepted December 9, 2002
Monitoring Editor: Tony Hunter

Oxidative stress induces in endothelial cells a quick and transient coactivation of both stress-activated protein kinase-2/p38 and extracellular signal-regulated kinase (ERK) mitogen-activated protein kinases. We found that inhibiting the ERK pathway resulted, within 5 min of oxidative stress, in a misassembly of focal adhesions characterized by mislocalization of key proteins such as paxillin. The focal adhesion misassembly that followed ERK inhibition with the mitogen-activated protein kinase kinase (MEK) inhibitor PD098059 (2′-amino-3′-methoxyflavone) or with a kinase negative mutant of ERK in the presence of $H_2O_2$ resulted in a quick and intense membrane blebbing that was associated with important damage to the endothelium. We isolated by two-dimensional gel electrophoresis a PD098059-sensitive phosphoprotein of 38 kDa that we identified, by mass spectrometry, as tropomyosin-1. In fact, $H_2O_2$ induced a time-dependent phosphorylation of tropomyosin that was sensitive to inhibition by PD098059 and UO126 (1,4-diamino-2,3-dicyano-1,4-*bis*[2-aminophenylthio]butanediane). Tropomyosin phosphorylation was also induced by expression of a constitutively activated form of MEK1 ($MEK^{CA}$), which confirms that its phosphorylation resulted from the activation of ERK. In unstimulated cells, tropomyosin-1 was found diffuse in the cells, whereas it quickly colocalized with actin and stress fibers upon stimulation of ERK by $H_2O_2$ or by expression of $MEK^{CA}$. We propose that phosphorylation of tropomyosin-1 downstream of ERK by contributing to formation of actin filaments increases cellular contractility and promotes the formation of focal adhesions. Incidentally, ML-7 (1-[5iodonaphthalene-1-sulfonyl]homopiperazine, HCl), an inhibitor of cell contractility, inhibited phosphorylation of tropomyosin and blocked the formation of stress fibers and focal adhesions, which also led to membrane blebbing in the presence of oxidative stress. Our finding that tropomyosin-1 is phosphorylated downstream of ERK, an event that modulates its interaction with actin, may lead to further understanding of the role of this protein in regulating cellular functions associated with cytoskeletal remodeling.

Article published online ahead of print. Mol. Biol. Cell 10.1091/mbc.E02–04–0235. Article and publication date are at www.molbiolcell.org/cgi/doi/10.1091/mbc.E02–04–0235.

¶ Corresponding author. E-mail address: jacques.huot@phc.ulaval.ca.

Abbreviations used: ERK, extracellular signal-regulated kinase; FITC, fluorescein isothiocyanate; HSP, heat shock protein; HUVEC, human umbilical vein endothelial cell; MALDI-TOF, matrix-assisted laser desorption/time of flight; MAP, mitogen-activated protein; MLCK, myosin light chain kinase; PAEC, porcine aortic endothelial cells; SAPK2/p38, stress-activated protein kinase-2/p38; ML-7, (1-[5iodonaphthalene-1-sulfonyl]homopiperazine, HCl); PD098059, 2′-amino-3′-methoxyflavone; UO126, (1,4-diamino-2,3-dicyano-1,4-*bis*[2-aminophenylthio]butanediane); SB203580, 4-(4-fluorophenyl)-2-(4-methylsulfinylphenyl)-5-(pyridyl)1H-imidazole).

## INTRODUCTION

Actin polymerization and remodeling are centrally involved in many cellular functions that include motility, migration, division, endocytosis, and gene expression. They also contribute to apoptosis and pathological processes such as inflammation and cardiac hypertrophy. Regulation of actin organization and dynamics is a highly complex process that involves a number of actin-binding proteins, including capping, branching, severing, sequestering, and cross-linking proteins. Actin homeostasis further involves binding to membrane-anchoring proteins located in focal adhesion sites. Focal adhesions are sites of cell attachment to the extracellular matrix. Their assembly is induced by increased cellular contractility and is characterized by the recruitment of signaling molecules such as focal adhesion kinase and paxillin, and of structural and membrane actin-anchoring proteins such as vinculin and tensin (Chrzanowska-Wodnicka and Burridge, 1996; Ridley, 1999; Turner, 2000). These proteins provide a link allowing the anchorage of stress fibers to the membrane and to integrins. All the actin-binding proteins are under the regulation of a complex network of bidirectional outside-in and inside-out signaling cascades that integrate the signals that lead to the proper organization and dynamics of the microfilament cytoskeleton.

Tropomyosins encompass a large family of actin regulatory proteins that are expressed by muscle and nonmuscle cells. Nonmuscle cells express multiple isoforms of tropomyosin that are encoded by a combination of multiple genes some of which contain alternative promoters and some of which exhibit alternative splicing of primary mRNA transcripts (Lees-Miller and Helfman, 1991). The various forms of nonmuscle tropomyosins are regrouped into high- (~34–40 kDa, e.g., TM1, TM2, TM3, and TM6) and low-molecular-weight tropomyosin isoforms (~28–32 kDa, e.g., TM5) (Warren *et al.*, 1995). A dynamic balance between the low- and high-molecular-weight tropomyosin tightly regulates microfilament organization. For instance, the transition of lens epithelial cells, from the undifferentiated to the differentiated state, is characterized by a shift in tropomyosin isoform expression from high molecular weight to low molecular weight and by a resulting reorganization of actin, from stress fibers to cortical F-actin (Fischer *et al.*, 2000). The mechanisms by which tropomyosin contributes to regulate the integrity of the microfilament organization and functions are still ill defined. The lower molecular weight tropomyosins have a weaker actin-binding capacity than the high-molecular-weight tropomyosins. They are found in both ruffles and stress fibers, whereas the high-molecular-weight tropomyosins are found mostly in stress fibers (Lees-Miller and Helfman, 1991). The low-molecular-weight isoforms are mostly involved in the regulation of motile process, whereas the high-molecular-weight isoforms are implicated in microfilament protection and organization (Warren *et al.*, 1995). In vitro, the high-molecular-weight isoforms of tropomyosin protect actin filaments against severing by gelsolin. In vivo, tropomyosin-1 null yeasts have less stable actin bundles (Ishikawa *et al.*, 1989; Liu and Bretscher, 1989). The nonmuscle cell tropomyosin-mediated modulation of actin properties underlies the regulation of basal cellular functions such as cell division, cell migration, extension of neuronal growth cone, movement of cytoplasmic organelles, and protein sorting (Pelham *et al.*, 1996; Gunning *et al.*, 1998; Lee *et al.*, 2000; Wong *et al.*, 2000). Tropomyosins possess multiple potential phosphorylatable sites that seem to be involved in modulating association with actin (Watson *et al.*, 1988; Sano *et al.*, 2000). In rabbit striated muscle, phosphorylation of $\alpha\alpha$-tropomyosin is associated with increased myosin $Mg^{2+}$/ATPase activity in vitro (Heeley *et al.*, 1989). A 250-kDa kinase responsible for phosphorylating tropomyosin in chicken embryo has been described previously (de-Belle and Mak, 1987). However, nothing more is known concerning the kinases and phosphatases that regulate the phosphorylation status of tropomyosins. Interestingly, tropomyosins are among the most abundant cytoskeletal proteins in various types of endothelial cells (Patton *et al.*, 1990). This suggests that they play important roles in regulating the numerous functions of endothelial cells associated with cytoskeletal remodeling.

Membrane blebbing is an early manifestation of toxicity both in vitro and in vivo (Gores *et al.*, 1990). It typically results from alterations of the microfilament organization in response to insult. Notably, membrane blebbing is associated with new actin polymerization, increased actin-myosin contractile force, and loss of focal adhesions (Mills *et al.*, 1998; Leverrier and Ridley, 2001; Kanthou and Tozer, 2002). In endothelial cells exposed to oxidative stress, disruption of focal adhesion assembly by chemical inhibition of the extracellular signal-regulated kinase (ERK) mitogen-activated protein (MAP) kinase pathway results in a quick and intense membrane blebbing activity that requires stress-activated protein kinase-2/p38 (SAPK2/p38)-heat shock protein (HSP)27-mediated enhanced polymerization of F-actin (Huot *et al.*, 1998). Membrane blebbing is associated with cytoplasmic and nuclear manifestations of apoptosis, and depending on the cellular context may be caspase dependent or caspase independent (McCarthy *et al.*, 1997; Huot *et al.*, 1998; Lavoie *et al.*, 2000; Coleman *et al.*, 2001; Sebbagh *et al.*, 2001). In addition to its role in apoptosis, membrane blebbing may have deleterious consequences in vivo. In endothelial cells, membrane blebbing leads to a narrowing of the vascular lumen associated with increased vascular resistance, which may ultimately lead to cardiac failure (Becker and Ambrosio, 1987). Bleb shedding from ischemic renal tubule cells may lead to tubular obstruction (Phelps *et al.*, 1989). In liver, bleb shedding from hepatocytes seems to be responsible for the release in the bloodstream of viral antigens such as hepatitis B (Gores *et al.*, 1990).

In the present study, we report, for the first time, that tropomyosin-1 is phosphorylated downstream of ERK either after exposure to $H_2O_2$ or by expression of a constitutively activated form of mitogen-activated protein kinase kinase $(MEK)^{CA}$. We also present evidence suggesting that the phosphorylation of tropomyosin-1 regulates its association with F-actin and that it is required for the proper assembly of focal adhesion, and for the bundling and anchorage of F-actin into stress fibers. When phosphorylation of tropomyosin-1 is impaired by ERK inhibition with PD098059 (2′-amino-3′-methoxyflavone) or by a dominant negative form of ERK, focal adhesion assembly is impaired, which results in membrane blebbing and damage to the endothelial barrier and increased permeability.

## MATERIALS AND METHODS

### *Materials*

$H_3[^{32}P]O_4$ was purchased from Amersham Biosciences (Montréal, QC, Canada). $H_2O_2$, fluorescein isothiocyanate (FITC)-phalloidin, ML-7 (1-[5iodonaphthalene-1-sulfonyl]homopiperazine, HCl), and endothelial cell growth supplement were from Sigma-Aldrich (Oakville, ON, Canada). PD098059 and UO126 (1,4-diamino-2,3-dicyano-1,4-*bis*[2-aminophenylthio]butanediane) were purchased from Calbiochem (San Diego, CA) and Promega (Madison, WI), respectively, and were diluted in dimethyl sulfoxide (DMSO) to make stock solutions of 20 mM. Chemicals for electrophoresis were obtained from Bio-Rad (Mississauga, ON, Canada) and Fisher Scientific (Montréal, QC, Canada).

### *Antibodies*

Anti-paxillin mouse antibody was purchased from BD Transduction Laboratories (Mississauga, ON, Canada). Anti-Myc tag (9E10) and anti-hemagglutinin (HA) tag (12Ca5) mouse antibodies were gifts

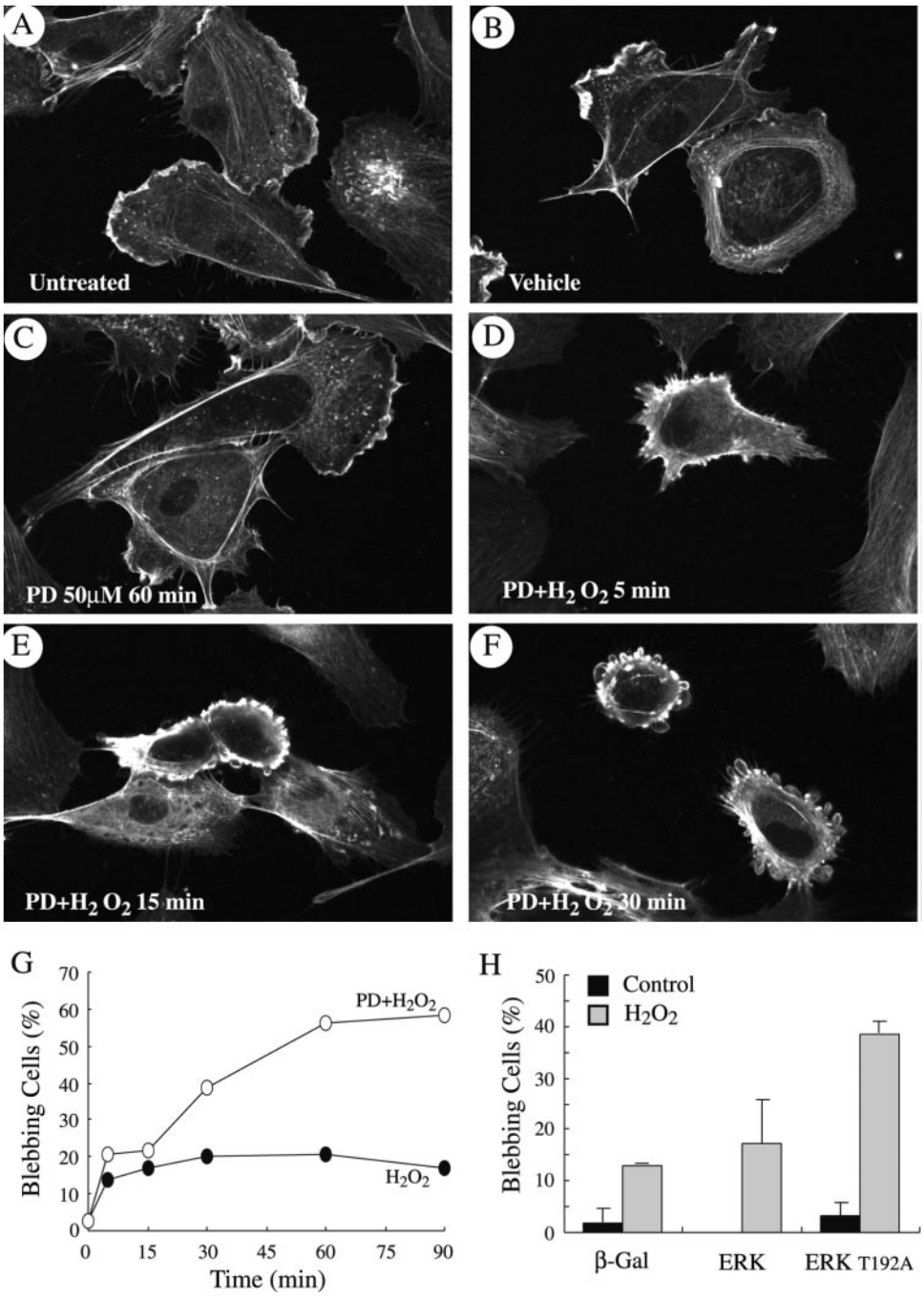


**Figure 1.** Inhibition of ERK MAP kinase in the presence of $H_2O_2$ leads to early membrane blebbing. Exponentially growing HUVECs were either untreated (A) or treated with vehicle alone (0.25% DMSO, 60 min; B) or they were pretreated with the MEK inhibitor PD098059 (50 $\mu$M) for 60 min and treated or not (C) with 250 $\mu$M $H_2O_2$ for 5 min (D), 15 min (E), or 30 min (F). In G, exponentially growing HUVECs were pretreated with vehicle (0.25% DMSO, 60 min; filled circles) or with PD098059 (50 $\mu$M, 60 min; unfilled circles) and then were treated with 250 $\mu$M $H_2O_2$ for increasing periods of times. Blebbing cells were visualized by fluorescence microscopy, counted, and means from two separate experiments were calculated. In H, PAECs were transfected with vector expressing either $\beta$-galactosidase, wild-type ERK1 MAP kinase fused to HA tag, or kinase dead ERK1T192A MAP kinase fused to HA tag. To make sure that MAP kinase kinase upstream of ERK was not limiting, transfection with ERK1 was supplemented with vector-expressing wild-type MEK1. Cells were treated (gray bars) or not (black bars) with 500 $\mu$M $H_2O_2$ for 60 min. Blebbing HA-stained cells were visualized by fluorescence microscopy, counted, and means from two separate experiments were calculated. Membrane blebbing has been quantitated by counting the number of blebbing cells over a total of 500 cells counted in different representative fields. In each experiment, cells were fixed, permeabilized, and stained for F-actin by using FITC-phalloidin and for HA tag by using 12Ca5 antibody (H only) as described in MATERIALS AND METHODS.

from Dr. Jacques Landry (Université Laval, Québec). Anti-ERK2 is a rabbit polyclonal antibody raised against a synthetic peptide that corresponds to the 14 carboxy-terminal amino acids of rat ERK2 (Huot *et al.*, 1997). Anti-tropomyosin monoclonal mouse antibody was purchased from Sigma-Aldrich. Anti-MEK1 #9 rabbit polyclonal antibody was a gift from Dr. Jean Charron (Université Laval, Québec). Monoclonal and polyclonal anti-phospho-ERK antibodies were purchased from Cell Signaling Technology (Beverly, MA).

### *Cells*

Human umbilical vein endothelial cells (HUVECs) were isolated by collagenase digestion of umbilical veins from undamaged sections of fresh cords (Huot *et al.*, 1997). Briefly, the umbilical vein was cannulated, washed with Earle's balanced salt solution, and perfused for 10 min with collagenase (1 mg/ml) in Earle's balanced salt solution at 37°C. After perfusion, the detached cells were collected, the vein was washed with 199 medium, and the wash-off was pooled with the perfusate. The cells were washed by centrifugation and plated on gelatin-coated 75-$cm^2$ culture dishes in 199 medium containing 20% heat-inactivated fetal bovine serum, endothelial cell growth supplement (60 $\mu$g/ml), glutamine, heparin, and antibiotics. Replicated cultures were obtained by trypsinization and were used at passages <5. The identity of HUVECs as endothelial cells was confirmed by their polygonal morphology and by detecting their immunoreactivity for factor VIII-related antigens. Porcine aortic endothelial cells (PAECs) were cultivated in F-12 medium containing 10% fetal calf serum. Cultures were incubated at 37°C in a humidified atmosphere containing 5% $CO_2$.

### *Plasmids and Adenoviral Vectors*

Plasmid pCH110, expressing $\beta$-galactosidase, was purchased from Amersham Biosciences. Plasmid pcDNANeo-HAP-Mapk was a gift from Dr. Sylvain Meloche (IRCM, Montréal) and expresses wild-type human MAP kinase ERK1 fused to HA tag. Plasmids pcDNA-Neo-MapkT192A and pECE-HA-Mapkk were a gift from Dr. Jacques Pouysségur (Institute of Signaling, Nice, France) and express human ERK1 kinase dead and the wild-type human MAP kinase kinase MEK1, respectively, and are both fused to HA tag. Adenoviral vectors carrying $\beta$-galactosidase and constitutively active MEK1 ($MEK^{CA}$) were given by Drs. Claude Gravel (Université Laval, Québec) and Sakae Tanaka (University of Tokyo, Tokyo, Japan) (Miyazaki *et al.*, 2000), respectively.

### *Gene Transfer*

Exponentially growing PAECs were plated 24 h before lipofection (10,000 cells/Lab-Tek well). Cells were incubated with 55 ng of plasmids expressing $\beta$-galactosidase, ERK1, or ERKT192A kinase dead along with 55 ng of plasmid expressing MEK1 with a ratio of 4:1 of Tfx50 (Promega) for 2 h in the absence of serum. Cells were then overlaid with 0.5 ml of complete medium, and assays were done 24 h posttransfection. In HUVECs, gene transfer was achieved by using adenoviral constructs containing LacZ or $MEK^{CA}$ genes. Briefly, HUVECs were plated for 24 h before the addition for 6 h of adenoviral vector suspensions to the monolayers of HUVEC cultures. The infection media were then changed for fresh media. Sixteen to 48 h later, depending on the experiments, the cells, whose 80% expressed the protein, were treated and used for experiments

### *Immunoprecipitation*

After treatments, cells were lysed in 75 $\mu$l of buffer B (150 mM NaCl, 50 mM Tris-HCl pH 7.5, 1% Triton X-100, 0.1% sodium deoxycholate, 2 mM EDTA, 2 mM EGTA, 1 mM $Na_3VO_4$, 1 mM leupeptin, 50 $\mu$g/ml pepstatin, and 1 mM phenylmethylsulfonyl fluoride [PMSF]). Samples were diluted three times and precleared with 10 $\mu$l of a 50% (vol/vol) protein G-Sepharose suspension for 15 min with shaking on ice. Supernatants were incubated on ice for 90 min

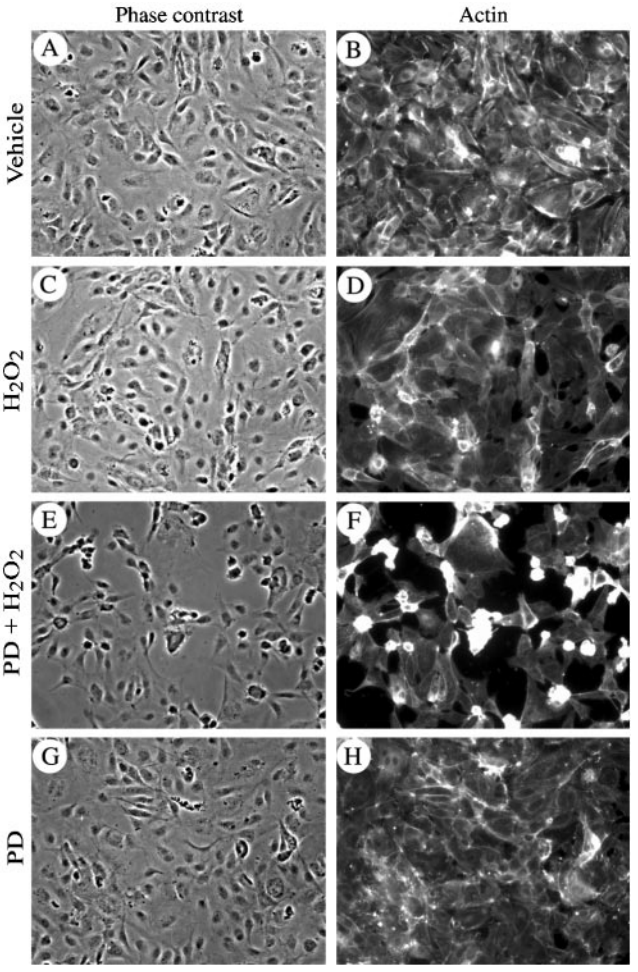


**Figure 2.** Inhibition of ERK MAP kinase in the presence of $H_2O_2$ is associated with disruption of the endothelial layer. HUVECs ($4 \times 10^4$) were plated in Lab-Tek chambers and grown to confluence (72 h). They were then pretreated with vehicle (0.25% DMSO, 60 min; A–D) or with PD098059 (50 $\mu$M, 60 min; E–H) and thereafter were treated or not (A, B, G, and H) with 250 $\mu$M $H_2O_2$ for 30 min (C–F). After treatments, cells were fixed, permeabilized, and stained for F-actin by using FITC-phalloidin as described in MATERIALS AND METHODS. Endothelial layers were visualized at 20× magnification by phase contrast (A, C, E, and G) and by fluorescence microscopy after staining for F-actin (B, D, F, and H).

with 8 $\mu$l of mouse monoclonal anti-tropomyosin antibody, and then 10 $\mu$l of 50% (vol/vol) protein G-Sepharose (Amersham Biosciences) was added and incubation was extended for 30 min on ice with shaking. Antibody–antigen complexes were washed four times with buffer B and then SDS-PAGE loading buffer was added. Proteins were separated through SDS-PAGE, and the gel was dried or transferred onto nitrocellulose for Western blotting by using anti-tropomyosin.

### *Kinase Assays*

ERK kinase activity was assayed in immune complexes after immunoprecipitation of cell extracts by using the rabbit polyclonal anti-

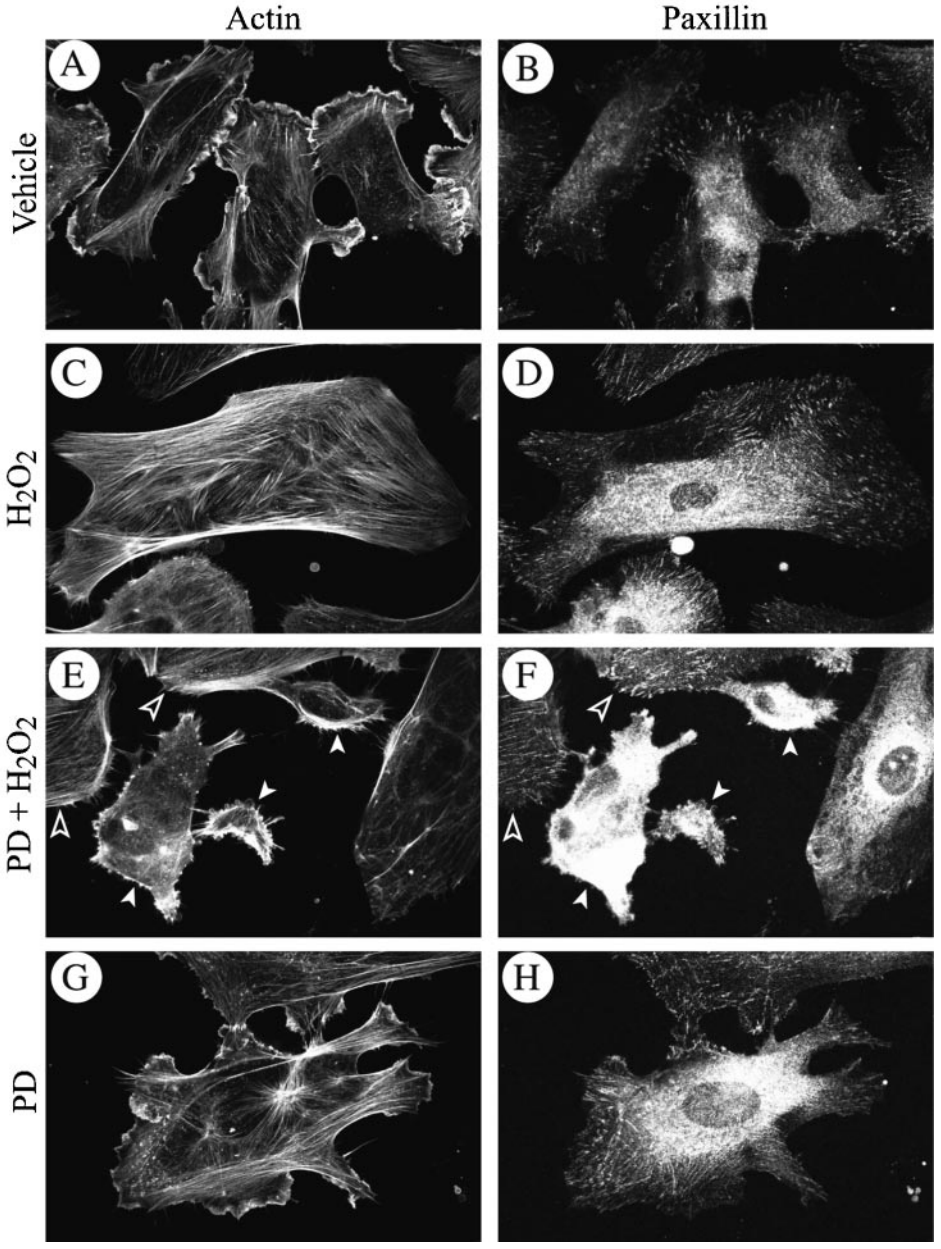


**Figure 3.** Early membrane blebbing is associated with focal adhesion misassembly. Exponentially growing HUVECs were pretreated with vehicle (0.25% DMSO, 60 min; A–D) or with PD059098 (50 $\mu$M, 60 min; E–H), and then they were treated or not (A, B, G, and H) with 250 $\mu$M $H_2O_2$ for 5 min; (C–F). After treatments, cells were fixed, permeabilized, and stained for F-actin by using FITC-phalloidin and for paxillin by using anti-paxillin monoclonal antibody as described in MATERIALS AND METHODS. Open arrowheads show intact cells and white arrow heads show cells that begin to bleb.

ERK2 (Huot *et al.*, 1997). The assays were carried out in 25 $\mu$l of kinase buffer K: 100 $\mu$M ATP, 3 $\mu$Ci of [$\gamma$-$^{32}$P]ATP (3000 Ci/mmol), 40 mM *p*-nitrophenyl phosphate, 20 mM 3-(*N*-morpholino)propanesulfonic acid pH 7, 10% glycerol, 10 mM $MgCl_2$, 0.05% Triton X-100, 1 mM dithiothreitol, 1 mM leupeptin, 0.1 mM PMSF. The kinase activity was assayed for 30 min at 30°C and was stopped by the addition of 10 $\mu$l of SDS-PAGE loading buffer. Immunoprecipitated ERK2 was assayed using myelin basic protein as substrate (Huot *et al.*, 1997) and was evaluated by measuring incorporation of the radioactivity into the specific substrates after resolution by SDS-PAGE and quantification using PhosphorImager (Molecular Dynamics, Sunnyvale, CA). ERK activity has also been evaluated by Western blotting with monoclonal anti-phospho ERK antibody (Cell Signaling Technology) that recognizes the phosphorylated form of ERK.

### *In Vivo Phosphorylation*

HUVECs plated in 35-mm Petri dishes were incubated in $PO_4$-free medium for 1 h before being labeled with $H_3[^{32}P]O_4$ (60–200 $\mu$Ci/ml) for 90 min. Cells were treated and were extracted in IEF buffer (3.4% CHAPS, 1.2 M $\beta$-mercaptoethanol, 2.7% ampholytes 4–6, 0.7% ampholytes 3–10, 17 mM NaF, 1.7 mM EDTA, 1.7 mM PMSF, 1 mM $Na_3VO_4$, 15 M urea) for two-dimensional (2D) separation, or in buffer B for immunoprecipitation experiments. In some experiments, NaF (1 mM for 1 h) was added to the incubation medium to inhibit phosphatases and to allow the accumulation of phosphorylated tropomyosin. It has been shown that endothelial cells remain 100% viable after 2-h treatment to concentrations of NaF up to 20 mM (Wang *et al.*, 2001).

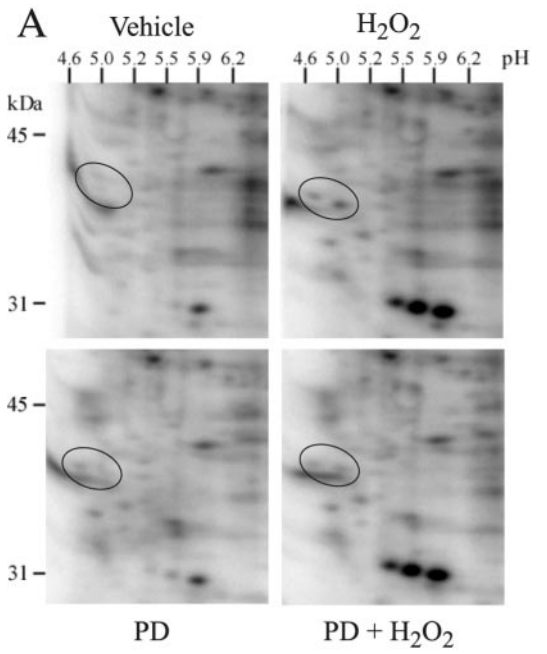


B

| Fragments | Fragment masses | |
|---|---|---|
| | Obtained | Expected |
| IQLVEEELDRAQER | 1727.94 | 1727.89 |
| MELQEIQLKEAK | 1475.74 | 1475.78 |
| EAETRAEFAER | 1308.63 | 1308.62 |
| TEERAELAESK | 1262.57 | 1262.62 |
| IQLVEEELDR | 1243.63 | 1243.65 |
| AEFAERSVAK | 1107.53 | 1107.58 |
| HIAEEADR | 940.46 | 940.45 |
| QAEERSK | 847.46 | 847.43 |

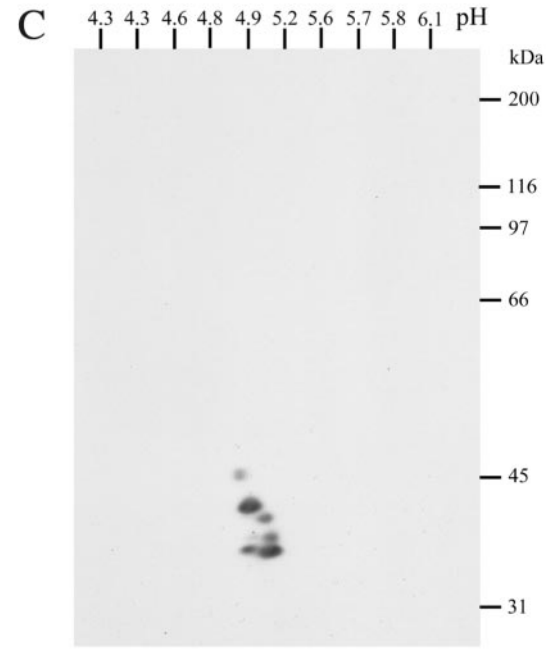


## 2D Gel Electrophoresis

After in vivo phosphorylation, cells were extracted in IEF buffer and were run for 16 h into pH 4.0–6.0 isofocusing electrophoresis gels. Gels were incubated for 10–15 min in loading buffer before being run into 8.5% SDS-PAGE. Gels were dried and exposed for imaging with PhosphorImager (Molecular Dynamics). Control gels run similarly, but not dried, were used to cut the spots of interest on the exposed gels. To further separate the tropomyosin isoforms, cells extracted in IPG buffer (7 M urea, 4% CHAPS, 20 mM EDTA, 0.5% IPG buffer pH 4.5–5.5) were run overnight on 18-cm Immobilon Drystrip pH 4.5–5.5 on an IPGPhor (Amersham Biosciences). Thereafter, gels were run into 8.5% SDS-PAGE, transferred onto nitrocellulose membranes, and processed for immunodetection.

## Mass Spectrometry Analysis

Mass spectrometry was performed by Dr. Nick Morrice (Medical Research Council Protein Phosphorylation Unit, University of Dundee, Dundee, United Kingdom). Tryptic peptides were analyzed on an Elite STR matrix-assisted laser desorption/time of flight (MALDI-TOF) mass spectrometer (Applied Biosystems, Foster City, CA) with saturated $\alpha$-cyanocinnamic acid as the matrix. The mass spectrum was acquired in the reflector mode and was internally mass calibrated. The tryptic peptide ions obtained were scanned against the Swiss-Prot and Genpep databases by using the MS-FIT program of Protein Prospector developed by Karl Clauser and Peter Baker (http://proteomics.biotech.vt.edu/ucs/html4.0/instruct/Fitman.htm).

## Fluorescence Microscopy

Confocal microscopy was used for immunofluorescence visualization of F-actin, tropomyosin, paxillin, and phospho-ERK (Huot *et al.*, 1997). The cells were plated on gelatin-coated Lab-Tek (Nalge Nunc, Naperville, IL) dishes. After treatment, they were fixed with 3.7% formaldehyde and permeabilized with 0.1% saponin in phosphate-buffered saline, pH 7.5. F-actin was detected using FITC-conjugated phalloidin (33.3 $\mu$g/ml) diluted 1:50 in phosphate buffer. Appropriate antibodies were used for antigen staining. Antigen–antibody complexes were detected with biotin-labeled anti-mouse IgG and were revealed with Texas Red-conjugated streptavidin. The cells were examined by confocal microscopy with an MRC-1024 imaging system (Bio-Rad) mounted on a Diaphot-TDM (Nikon, Tokyo, Japan) equipped with a 60× objective lens with a 1.4 numerical aperture (Huot *et al.*, 1997). For triple labeling, antigen–antibody complexes were detected using anti-mouse IgG antibody coupled to FITC, anti-rabbit IgG antibody coupled to AMCA (7-amino-4-methyl-coumarin-3-acetic acid), whereas F-actin was detected using rhodamine-phalloidin. The cells were examined under fluorescent microscopy with an Eclipse E600 (Nikon) equipped with a 40× 0.85

**Figure 4.** MALDI-TOF identification of tropomyosin-1 as a downstream target of ERK. (A) Exponentially growing HUVECs were labeled with $H_3[^{32}P]O_4$ and were pretreated with vehicle (0.25% DMSO, 60 min; top) or with PD098059 (50 $\mu$M, 60 min; bottom). They were then treated or not (left) with 250 $\mu$M $H_2O_2$ for 15 min (right). Proteins were extracted and run into IEF (pH 4–6) gels and in a second dimension into 8.5% SDS-PAGE. Representative autoradiograms from four separate experiments are shown. (B) In a separate experiment, spots circled in A were excised and processed for MALDI-TOF analysis. Database searching identified the protein as tropomyosin-1 with eight matching peptides that represent 23% sequence coverage. In C, exponentially growing HUVECs were extracted and processed for 2D electrophoresis as in A. The gel was transferred on nitrocellulose membrane and processed for immunodetection by using a monoclonal anti-tropomyosin antibody that cross-reacted with the different isoforms of tropomyosin.

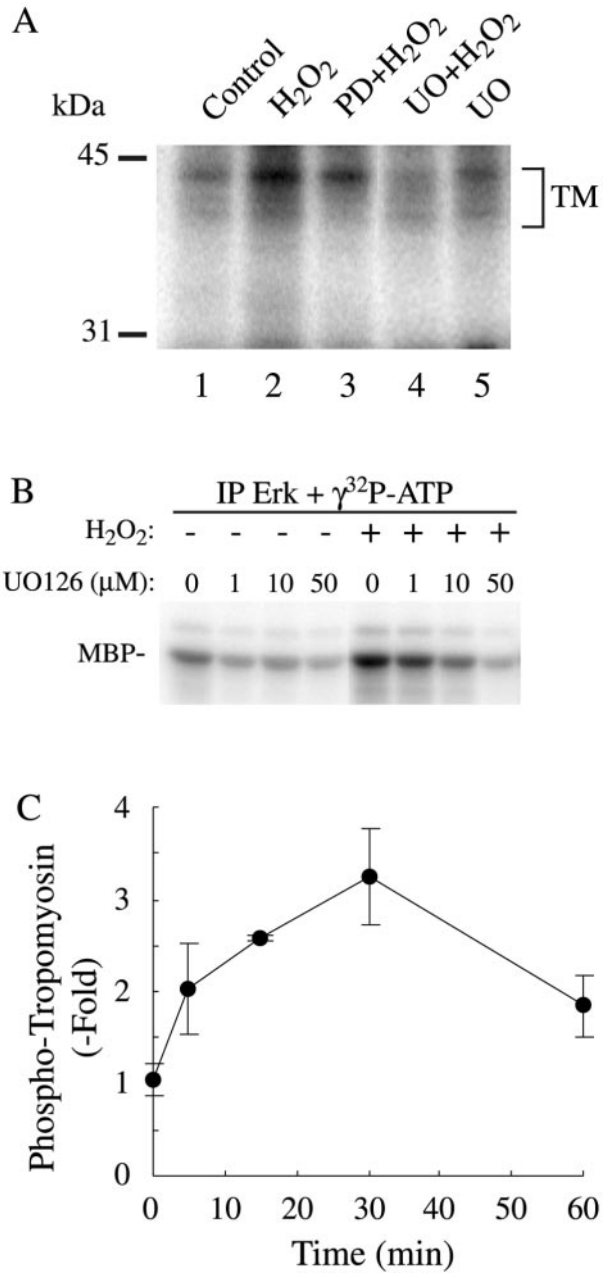


**Figure 5.** $H_2O_2$ induces a time-dependent phosphorylation of tropomyosin that is inhibited by inhibitors of the ERK pathway. (A) Exponentially growing HUVECs were labeled with $H_3[^{32}P]O_4$ and were pretreated simultaneously with the phosphatase inhibitor NaF (1 mM) and with vehicle (0.25% DMSO, 60 min; lanes 1 and 2), or with PD098059 (50 $\mu$M, 60 min; lane 3) or with UO126 (50 $\mu$M, 60 min; lanes 4 and 5) and treated for 30 min with 250 $\mu$M $H_2O_2$ (lanes 2–4). Proteins were extracted, immunoprecipitated using anti-tropomyosin antibody, and antigen–antibody complexes were run into 8.5% SDS-PAGE. Representative autoradiogram from two separate experiments is shown. (B) Exponentially growing HUVECs were pretreated with vehicle (0.25% DMSO, 60 min) or for 60 min with increasing concentration of MEK inhibitor UO126 and treated or not with 500 $\mu$M $H_2O_2$ for 30 min. After treatment, cells were extracted and processed for ERK kinase assay using myelin basic protein as substrate as described in MATERIALS AND METHODS. (C) Exponentially growing HUVECs were labeled with $H_3[^{32}P]O_4$ and were pretreated with vehicle (0.25% DMSO, 60 min) along with phosphatase inhibitor NaF (1 mM) and were treated for increasing time with 250 $\mu$M $H_2O_2$. Proteins were extracted and immunoprecipitated using mouse monoclonal anti-tropomyosin antibody. Antigen–antibody complexes were run into 8.5% SDS-PAGE, and tropomyosin bands were quantified using PhosphorImager. Means with error bars from three separate experiments are shown.

numerical aperture objective lens. Images were captured as 16-bit TIFF files with a Micromax 130 YHS cooled (−30°C) camera (Princeton Instruments, Trenton, NJ) driven by MetaMorph software (Universal Imaging, Downingtown, PA).

## RESULTS

### *ERK Inhibition in Presence of Oxidative Stress Leads to Early Membrane Blebbing of Endothelial Cells and to Disruption of Endothelial Layer*

Oxidative stress induces in endothelial cells a quick and marked activation of the SAPK2/p38 and ERK MAP kinases (Huot *et al.*, 1997). Activation of SAPK2/p38 results in an increased actin polymerization and in a massive actin reorganization into transcytoplasmic stress fibers (Huot *et al.*, 1998; Figure 3C). In both cases, this depends on the phosphorylation of the actin-polymerizing factor HSP27 by mitogen-activated kinase kinase-activated protein kinase-2, a direct downstream target of SAPK2/p38 (Huot *et al.*, 1997, 1998). Intriguingly, polymerized F-actin could not assemble into stress fibers and remained at the periphery of the cells when $H_2O_2$-induced activation of ERK was inhibited with PD098059. In those conditions, small patches of actin began to form within 5 min (Figure 1, A–D), which quickly evolved in membrane blebbing with actin remaining at the periphery of the blebs (Figure 1, E and F). After 60 min of exposure to 250 $\mu$M $H_2O_2$, 40–60% of the cells, in which ERK was blocked with PD098059, exhibited intense membrane blebbing (Figure 1G). Yet, 95% of cells remained attached. Similar results were obtained in porcine aortic endothelial cells cotransfected with a wild-type MAP kinase kinase MEK1 and kdERK1, a mutant form of ERK1 that acts as dominant negative and suppresses 70% of both ERK1 and ERK2 activities in response to growth factors (Figure 1H; Pages *et al.*, 1993). Treating these transfected cells with $H_2O_2$ resulted in membrane blebbing in ~40% of the treated cells expressing kdERK1. In contrast, blebbing was found in only 12% of the $H_2O_2$ cells that were transfected with an irrelevant protein, $\beta$-galactosidase. As shown in Figure 2, membrane blebbing was associated with cell shrinking, dismantling of cell-cell contacts, and a marked increase in the interendothelial spaces in tight confluent cultures of HUVECs that mimic an in situ endothelial layer. The disruption of the endothelial layer after exposure to PD098050 plus $H_2O_2$ was associated with an approximately twofold increase in the transendothelial permeability to albumin of a layer of endothelial cells by using either a Boyden chamber or a perfused rat mesenteric venules as models (our unpublished data). Overall, these results indicated that ERK inhibition in the presence of oxidative stress induced early manifestations of endothelial toxicity that are characterized by membrane blebbing and loss of endothelial barrier integrity.

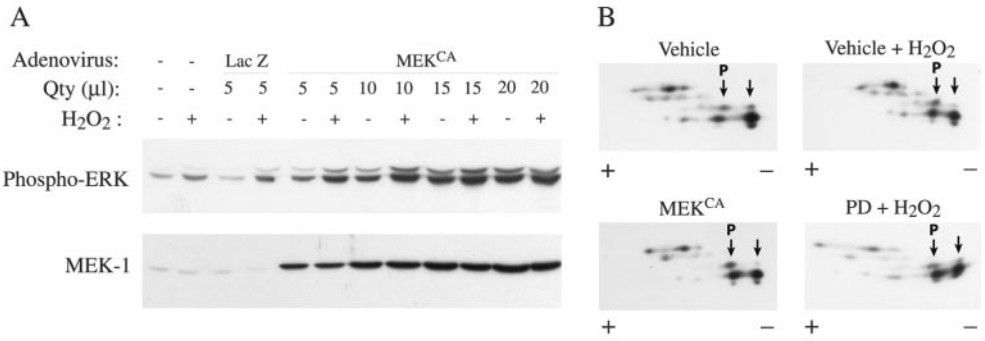


**Figure 6.** Tropomyosin is phosphorylated in cells in which ERK is activated by expression of a constitutive activated form of MEK1. (A) Exponentially growing HUVECs were infected or not with varying quantity of adenoviral vector carrying β-galactosidase or $MEK^{CA}$. Twenty-four hours later, cells were treated with 250 μM $H_2O_2$. Proteins were extracted, run into 8.5% SDS-PAGE, and transferred on nitrocellulose membrane. Immunodectections with monoclonal mouse anti-phospho-ERK antibody and rabbit polyclonal anti-MEK1 #9 antibody are shown. (B) Exponentially growing HUVECs were pretreated or not with vehicle (0.25% DMSO, 60 min) or with PD098059 (50 μM, 60 min; PD) and were treated or not for 30 min with 250 μM $H_2O_2$. Bottom left, exponentially growing HUVECs were infected with 15 μl of adenoviral vector carrying $MEK^{CA}$. Proteins were extracted in IPG buffer (pH 4.5–5.5) and separated on IPGPhor as described in MATERIALS AND METHODS. IEF gels were run into 8.5% SDS-PAGE for the second dimension. The gel was transferred on nitrocellulose membrane and processed for immunodetection with monoclonal anti-tropomyosin antibody that cross-reacted with the different isoforms of tropomyosin. Shift of the relevant tropomyosin-1 spots toward the acidic forms (P, phosphorylated) is indicated by arrows. Representative autoradiogram from two separate experiments is shown.

### *Early Membrane Blebbing Is Associated with a Defect in the Assembly of Focal Adhesions*

As shown in Figure 1, a major feature of membrane blebbing is that F-actin remains at the periphery of the cells and cannot assemble into stress fibers. In response to oxidative stress, bundling of actin into stress fibers is found in 70% of the cells, and it is associated with an increased actin polymerization and requires their anchorage to focal adhesions after the recruitment of focal adhesion proteins to the adhesion plaques. Inhibition of ERK with PD098059 did not inhibit the 1.5-fold increase in F-actin polymerization induced by $H_2O_2$ (our unpublished data), but it impaired the proper assembly of focal adhesion proteins at the ventral adhesion plaques. This is illustrated in Figure 3 that shows that in control cells and cells treated with PD098059, paxillin was found mainly at the base of lamellipodia (Figure 3, A, B, G, and H). In cells treated with $H_2O_2$, paxillin was recruited, within 5 min, to ventral adhesion plaques (Figure 3, C and D), whereas it was not recruited to and/or was lost from peripheral adhesions and remained diffuse in the cytoplasm in the cells that begin to bleb in the presence of PD098059 plus $H_2O_2$ (Figures 3, E and F; see white arrowheads). Overall, these findings suggest that membrane blebbing, when induced by oxidative stress in HUVECs in which ERK is inhibited, may result form a defect in the proper organization of focal adhesions. Of note, in contrast to previous findings in hepatocytes (Miyoshi *et al.*, 1996), the defect in the assembly of focal contacts that underlie membrane blebbing was independent of calpain activation. Indeed, neither $H_2O_2$ alone nor $H_2O_2$ in the presence of PD098059 increased the activity of calpain (our unpublished data).

### *Mass Spectrometry Identification of Tropomyosin-1 as a Downstream Target of ERK Activation by Oxidative Stress*

Because membrane blebbing induced by oxidative stress is associated with a misassembly of focal adhesions in cells in which ERK was inhibited, we hypothesized that the assembly of focal contacts in the presence of oxidative stress required the phosphorylation of a protein downstream of ERK. To verify this possibility, HUVECs labeled with $H_3[^{32}P]O_4$ were pretreated in the presence or not of PD098059 (50 μM for 60 min) and were treated or not with 250 μM $H_2O_2$ for 15 min. Proteins were extracted and separated by 2D gel electrophoresis. Thereafter, the gels were either stained to visualize the spots or dried and exposed for autoradiography. Among the spots phosphorylated by $H_2O_2$ and sensitive to inhibition by PD098059, two of them had a pI of ~4.9 and an $M_r$ of ~38 kDa (Figure 4A). They were pooled and analyzed by MALDI-TOF mass spectrometry. Data base searching indicate that the spots correspond to a single protein identified as tropomyosin-1 with eight matching peptides representing 23% of the sequence coverage and a MOWSE score >70 (Figure 4B). Western blotting by using an anti-tropomyosin antibody that cross-reacted with various isoforms of tropomyosin revealed six spots around a pI of 4.9 and 38 kDa. The two fastest migrating of these spots likely correspond to the spots of the autoradiogram that we have identified by mass spectrometry as tropomyosin-1 (Figure 4C). We next ascertained that tropomyosin was phosphorylated and that the phosphorylation resulted from ERK activation. HUVECs incubated with $H_3[^{32}P]O_4$ were treated or not for varying periods of time with $H_2O_2$ or $H_2O_2$ after UO126 or PD098059, two unrelated inhibitors of the ERK pathway (Figure 5, A–C; Huot *et al.*, 1998). Extracts were then prepared and tropomyosin-1 was immunoprecipitated and run into SDS-PAGE. Results showed that oxidative stress induces a threefold increase in the phosphorylation of tropomyosin that started at 5 min and was maximal at 30 min (Figure 5C). The $H_2O_2$-induced phosphorylation of tropomyosin was inhibited by inhibiting ERK, both with PD098059 or UO126, which was consistent with the fact that tropomyosin is a downstream target of ERK or of an ERK-dependent kinase (Figure 5, A and B). To further ascertain that tropomyosin was phosphorylated downstream of ERK, we performed 2D gel analysis and immunoblotting for total

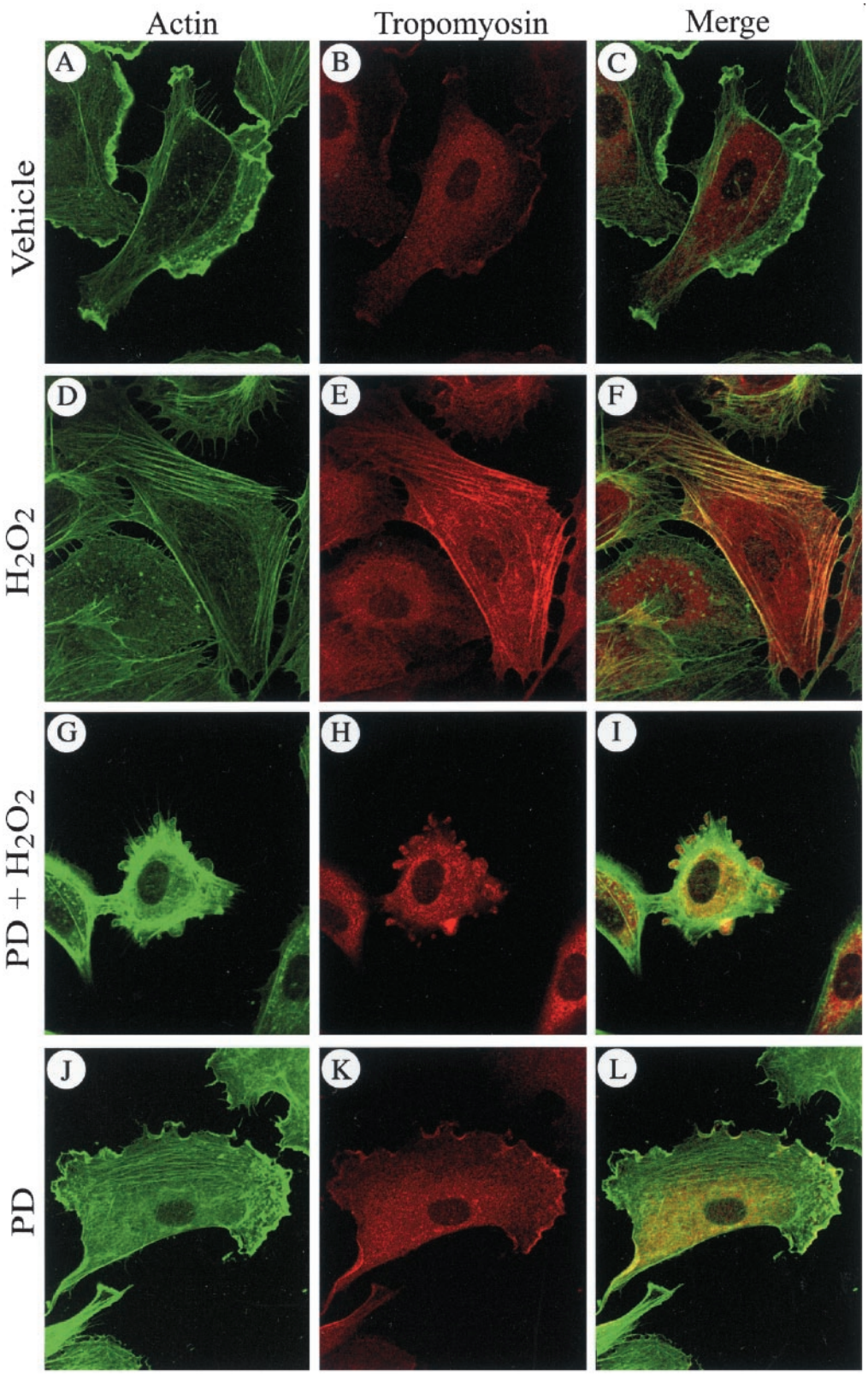
Actin
Tropomyosin
Merge
Vehicle
$H_2O_2$
PD + $H_2O_2$
PD
A
B
C
D
E
F
G
H
I
J
K
L

**Figure 7.**

tropomyosin in cells that have been treated with $H_2O_2$ in the presence or not or PD098059. We also made the same type of experiment in cells that express $MEK^{CA}$ after adenoviral-mediated infection. The results showed that, in control conditions, tropomyosin-1 exists under both nonphosphorylated and phosphorylated forms, which is consistent with our one-dimensional phosphorylation data. Treatment with $H_2O_2$ triggered a shift of the spot corresponding to nonphosphorylated tropomyosin-1 toward the acidic form, supporting its phosphorylation. The shift was blocked by PD098059, suggesting that it was ERK dependent (Figure 6B). Expression of $MEK^{CA}$ in concentration that increases to approximately fivefold the activity of ERK1/2 (Figure 6A), also induced a similar shift of tropomyosin toward the acidic form (Figure 6B). Together, these findings indicate that tropomyosin-1 is phosphorylated downstream of the ERK pathway in response to $H_2O_2$. From the 2D experiment we estimated to ~40% the amount of tropomyosin phosphorylated in response to $H_2O_2$, as well as by expression of $MEK^{CA}$.

### *ERK-mediated Phosphorylation of Tropomyosin-1 Is Associated with Formation of Stress Fibers*

Tropomyosin is known to associate with actin in vitro (Sen *et al.*, 2001; Cooper 2002). We thus, verified whether phosphorylation of tropomyosin-1 modulates its association with actin filaments in vivo. Cells were treated, fixed, permeabilized, and then processed for tropomyosin-1 and F-actin staining. We found that in control HUVECs, only small amount of tropomyosin was associated with actin at membrane ruffles (Figure 7, A–C, J–L). On treatment with $H_2O_2$, tropomyosin-1 is phosphorylated, which was accompanied with reorganization of the actin cytoskeleton into stress fibers. Tropomyosin-1 was then found along the actin stress fibers (Figure 7, D–F). In contrast, if activation of ERK is impaired with PD098059, tropomyosin is not phosphorylated and actin could not bundle into stress fibers. In those conditions, membrane blebbing is initiated and tropomyosin does not colocalize with actin being found at the periphery of the cells but outside of the blebs, whereas tropomyosin remains in the blebs (Figure 7, G–I). Interestingly, activation of ERK and phosphorylation of tropomyosin by expression of $MEK^{CA}$ was also associated with an increased formation of stress fibers and with the colocalization of tropomyosin with actin stress fibers in contrast to cells that express $\beta$-galactosidase (Figure 8, A–F). Notably, the staining of stress fibers for both actin and tropomyosin was more pronounced and fibrillar in the cells that exhibit the strongest staining for phospho-ERK taken as the reflect of $MEK^{CA}$ expression (Figure 8, B, D, and F; see arrows). In contrast, cells that do not stain for phospho-ERK do not exhibit stress fibers. Overall, these results suggest that ERK-mediated phosphorylation of tropomyosin-1 is involved in bundling of F-actin, possibly by favoring cross-linking of filamentous actin. This would increase cellular tension and promote the formation of focal adhesions and then the anchorage of actin filaments (Chrzanowska-Wodnicka and Burridge, 1996). We thus propose that phosphorylation of tropomyosin-1 downstream of ERK acts as a switch that contributes to increase cellular tension and then initiate the formation of focal adhesions and anchorage of elongating stress fibers. In this context, inhibiting cellular contractility shall be associated with impaired phosphorylation of tropomyosin and proper assembly of focal adhesion and lead to membrane blebbing in the presence of $H_2O_2$. We test this hypothesis by inhibiting cell contractility with ML-7, an inhibitor of myosin light chain kinase (MLCK) (Zhong *et al.*, 1998) that does not affect ERK activation by $H_2O_2$ (Figure 9G). As expected, treatments of the cells with ML-7 and $H_2O_2$ impaired, within 5 min, the $H_2O_2$-induced formation of stress fibers and recruitment of paxilllin to ventral focal adhesions (Figure 9, A–D). After 30 min, this was associated with a marked decrease in the phosphorylation of tropomyosin (Figure 9F) and with membrane blebbing in >65% of the cells (Figure 9E).

## DISCUSSION

In endothelial cells, oxidative stress induces an SAPK2/p38-mediated remodeling of the actin cytoskeleton that is characterized by increased actin polymerization and reorganization into stress fibers (Huot *et al.*, 1997). In the absence of a concomitant activation of the ERK pathway, focal adhesions do not assemble and polymerized actin generated through the SAPK2/p38 pathway cannot bundle into stress fibers and remains at the periphery of the cells (Huot *et al.*, 1998). This leads to an intense membrane blebbing that markedly alters the integrity of the endothelial layer. In the present study, we provided the first evidence that tropomyosin-1 was phosphorylated downstream of ERK. We also obtained results that suggest that ERK-mediated phosphorylation of tropomyosin-1 is required for the formation of stress fibers and for the proper assembly of focal adhesions in endothelial cells exposed to oxidative stress.

Focal adhesions are sites of tight adhesion between the membrane and the extracellular matrix on one hand, and the membrane and the cytoskeleton on the other. These structures provide a link allowing the anchorage of stress fibers to the membrane and to integrins. They are also the sites of an intense inside-out and outside-in signaling between adjacent cells and between the cells and the extracellular matrix (Geiger *et al.*, 2001). The findings that oxidative stress-induced misassembly of focal adhesions and membrane blebbing resulted from inhibition of ERK either by PD098059 or by expression of a dominant negative form of ERK indicate that ERK activation is essential for proper assembly of actin structures as well as focal adhesions. The rapidity at which ERK inhibition impairs

**Figure 7 (facing page).** Phosphorylation of tropomyosin-1 induces its colocalization with F-actin. Exponentially growing HUVECs were pretreated with vehicle (0.25% DMSO, 60 min; A–F) or with PD098059 (50 $\mu$M, 60 min; G–L), and then they were treated or not (A–C and J–L) with 250 $\mu$M $H_2O_2$ for 5 min (D–I). After treatments, cells were fixed, permeabilized, and stained for F-actin by using FITC-phalloidin and for tropomyosin by using anti-tropomyosin monoclonal antibody as described in MATERIALS AND METHODS. F-actin staining (A, D, G, and J), tropomyosin staining (B, E, H, and K and merged picture (C, F, I, and L) are shown. In merged picture, the yellow areas represent colocalization of both proteins. Representative fields from two separate experiments are shown.

the assembly of focal adhesions in the presence of oxidative stress is a strong suggestion that a protein phosphorylated downstream of ERK, rather than ERK-mediated neosynthesis of proteins, was involved in the assembly of focal contacts. The major contribution of our study is to have identified tropomyosin-1 as a target phosphorylated downstream of ERK and to have obtained results that suggest that its phosphorylation is associated with the assembly of focal contacts.

The identification of tropomyosin-1 as a downstream target of ERK has been obtained after mass spectrometry analysis of 2D gel electrophoresis spots that were phosphorylated by $H_2O_2$ in control HUVECs but not in HUVECs treated with PD098059. Thereafter, we obtained several experimental evidences supporting the point that tropomyosin-1 is phosphorylated downstream of ERK. First, the in vivo phosphorylation of tropomyosin in response to oxidative stress was markedly reduced by PD098059 and UO126, two unrelated inhibitors of ERK activation and activity, respectively; second, in 2D gel analysis, $H_2O_2$-induced a PD098059-sensitive shift of tropomyosin toward the acidic forms; third, a similar shift was induced by the expression of $MEK^{CA}$ in concentration that increased by fivefold the activity of ERK. It is thus unlikely that the phosphorylation of tropomyosin-1 by $H_2O_2$ resulted from an inhibition of phosphatases. In this context, vascular endothelial growth factor does not inhibit phosphatases but it induces a PD098059-sensitive phosphorylation of tropomyosin-1 (our unpublished data). Intriguingly, 2D gel analysis revealed that a pool of tropomyosin is phosphorylated under basal conditions. It is possible that this phosphorylated pool of tropomyosin reflects the basal level of activation of the ERK pathway. Tropomyosin-1 contains 13 serine and six threonine residues that can be putatively phosphorylated. However, none of these sites contain the minimum (S/TP) consensus sequence for phosphorylation by ERK, nor the FXP sequence that mediates the interaction of ERK with its substrates (Jacobs *et al.*, 1999). This suggests that ERK is unlikely to be the kinase that directly phosphorylates tropomyosin-1. Hence, tropomyosin-1 is phosphorylated by a kinase downstream of ERK but different from ERK. A tropomyosin kinase of 250,000 responsible for phosphorylating tropomyosin in chicken embryo has been described previously (deBelle and Mak, 1987). Whether this kinase is downstream of the ERK pathways remains, however, to be determined. Our finding that ML-7, a known inhibitor of MLCK, blocked the phosphorylation of tropomyosin, without having affected the activation of ERK, raised the possibility that MLCK or a kinase downstream of MLCK is the tropomyosin kinase. Incidentally, activated ERK2 can directly activate MLCK in vitro and MLCK has been shown to be a target of ERK after cell exposures to growth factors, to urokinase-type plasminogen activator, and after integrin engagement (Klemke *et al.*, 1997; Nguyen *et al.*, 1999; Finchman *et al.*, 2000).

Very little is known concerning the role of phosphorylated tropomyosin except that it seems to be involved in modulating association of myosin with actin and that its phosphorylation on S283 may increased the in vitro $Mg^{2+}$/ATPase of myosin (Watson *et al.*, 1988; Heeley *et al.*, 1989; Sano *et al.*, 2000). Herein, we obtained results that suggest that phosphorylation of tropomyosin might be a major determinant in bundling of F-actin in stress fibers and also in the assembly of focal contacts. The fact that phosphorylation of tropomyosin in the ERK pathway is involved in bundling of actin into stress fibers is suggested by the finding that after its phosphorylation by $H_2O_2$ or by expression of $MEK^{CA}$, tropomyosin colocalizes with F-actin along stress fibers. In contrast, when ERK-mediated phosphorylation is blocked with PD098059, the association between F-actin is impaired and no stress fiber is formed. Under these conditions, membrane blebbing is induced, with actin remaining at the periphery of the blebs and tropomyosin-1 remaining confined inside of the blebs. The incapacity of actin to bundle into stress fibers when ERK-mediated phosphorylation of tropomyosin is impaired might underlie focal adhesion misassembly and induction of membrane blebbing.

The current dogma concerning the formation of focal adhesions is that their assembly depends on the increased cellular tension and contractility generated through the enhanced actomyosin ATPase activity that results from the interaction between actin and myosin (Chrzanowska-Wodnicka and Burridge, 1996; Ridley, 1999; Watanabe *et al.*, 1999; Sastry and Burridge, 2000). In fact, agents that inhibit contractility, either by inhibiting MLCK or actin–myosin interactions, inhibit formation of stress fibers and assembly of focal adhesions (Chrzanowska-Wodnicka and Burridge, 1996). Accordingly, we found that ML-7, a potent inhibitor of cell contractility, impairs the phosphorylation of tropomyosin as well as the assembly of focal adhesions and leads to membrane blebbing in the presence of oxidative stress. A major mechanism underlying the increased cellular contractility implicates the phosphorylation of myosin light chain (MLC), through the RhoA pathway. Activation of this pathway increases the phosphorylation level of MLC via a direct phosphorylation cascade involving ROCK (Rhoa activated kinase)-MLCK and MLC or via an indirect mechanism by which it contributes to inhibit myosin phosphatase (Ridley and Hall, 1992; Amano *et al.*, 1996; Chrzanowska-Wodnicka and Burridge, 1996). MLC phosphorylation promotes the productive interaction of myosin heads with actin filaments, thus activating myosin ATPase and generating contractility. Increased myosin-actin contractility results in bundling of F-actin into stress fibers and triggers the assembly of focal adhesions (Chrzanowska-Wodnicka and Burridge, 1996; Sastry and Burridge, 2000). Intriguingly, tropomyosin is importantly involved in promoting the interaction between myosin and actin in various cell systems (Lees-Miller and Helfman, 1991). Moreover, phosphorylated $\alpha\alpha$tropomyosin increased in vitro the $Mg^{2+}$/ATPase activity of myosin (Heeley *et al.*, 1989), and activation of Rho kinase-directed pathways are critical for tropomyosin-1-mediated microfilament assemblies (Shah *et al.*, 2001). In accordance, we propose that ERK-mediated phosphorylation of tropomyosin-1 by facilitating the interaction between actin and myosin contributes to increase cell contractility and to bundling of actin into stress fibers. This is in line with our finding that after its phosphorylation, tropomyosin-1 colocalizes with stress fibers. This is also in line with our observation that ML-7 inhibits the phosphorylation of tropomyosin as well as the formation of stress fibers. ERK-tropomyosin–mediated forma-

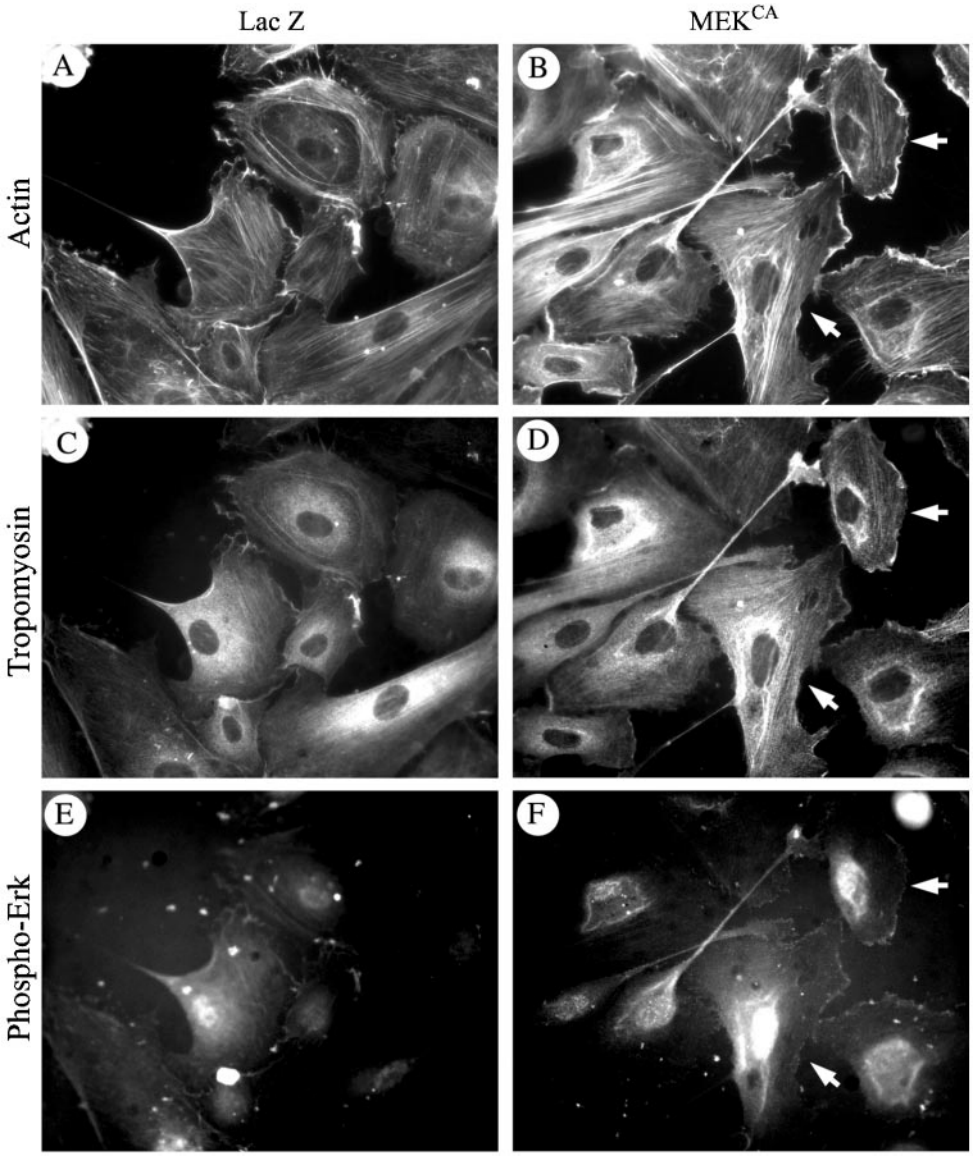


**Figure 8.** Phosphorylation of tropomyosin-1 by expression of $MEK^{CA}$ induces stress fiber formation and colocalization with F-actin. Exponentially growing HUVECs were infected with adenoviral vector carrying β-galactosisdase or $MEK^{CA}$. Forty-eight hours later, cells were fixed, permeabilized, and stained for F-actin by using rhodamine-phalloidin, for tropomyosin by using anti-tropomyosin monoclonal antibody, and for phospho-ERK (to monitor $MEK^{CA}$-expressing cells) by using anti-phospho-ERK polyclonal antibody. F-actin staining (A and B), tropomyosin staining (C and D), and phospho-ERK staining (E and F) are shown. Arrows indicate that cells that stain more strongly for phospho-ERK also stain more strongly for both fibrillar actin and tropomyosin. Representative fields from two separate experiments are shown.

tion of bundles of stress fibers and increase cellular tension will activate the integrin-associated mechanosensing processes, initiating the recruitment of focal adhesion proteins such as paxillin to the integrin complexes and then the assembly of focal adhesions (Riveline *et al.*, 2001).

Membrane blebbing is an early manifestation of toxicity that basically results from an imbalanced regulation of the cytoskeletal organization and dynamics (Mills *et al.*, 1999; Lavoie *et al.*, 2000; Kanthou and Tozer, 2002). In fact, membrane blebbing is strictly dependent on actin polymerization activity. It is blocked by cytochalasin D at a concentration that inhibits new actin polymerization without disrupting the actin filament network. It is also blocked by SB203580 that inhibits actin polymerization induced by the SAPK2/p38-HSP27 pathway (Huot *et al.*, 1998; Deschesnes *et al.*, 2001). Our finding that the intense blebbing activity that resulted from inhibition of ERK in cells exposed to $H_2O_2$ was associated with an accumulation of F-actin at the periphery of the cells and at the perimeter of the bleb is also consistent with the notion that blebbing is subsequent to cytoskeletal disturbances. Our observation that membrane blebbing is associated with a quick misassembly of focal adhesions induced by $H_2O_2$ suggests that disorganization of focal adhesions may be causal to the cytoskeletal disturbances that underlies membrane blebbing. This is in line with previous findings that show that oxidative stress-induced membrane blebbing in hepatocytes is associated with increased degradation of talin and α-actinin (Miyoshi *et al.*, 1996). Intriguingly, in certain cell types undergoing apoptosis, caspase activation induces the breakdown of the autoinhibitory domain of the RhoA kinase ROCK, which increased its activity and leads to phosphorylation of MLC and then to membrane blebbing (Mills *et al.*, 1998;

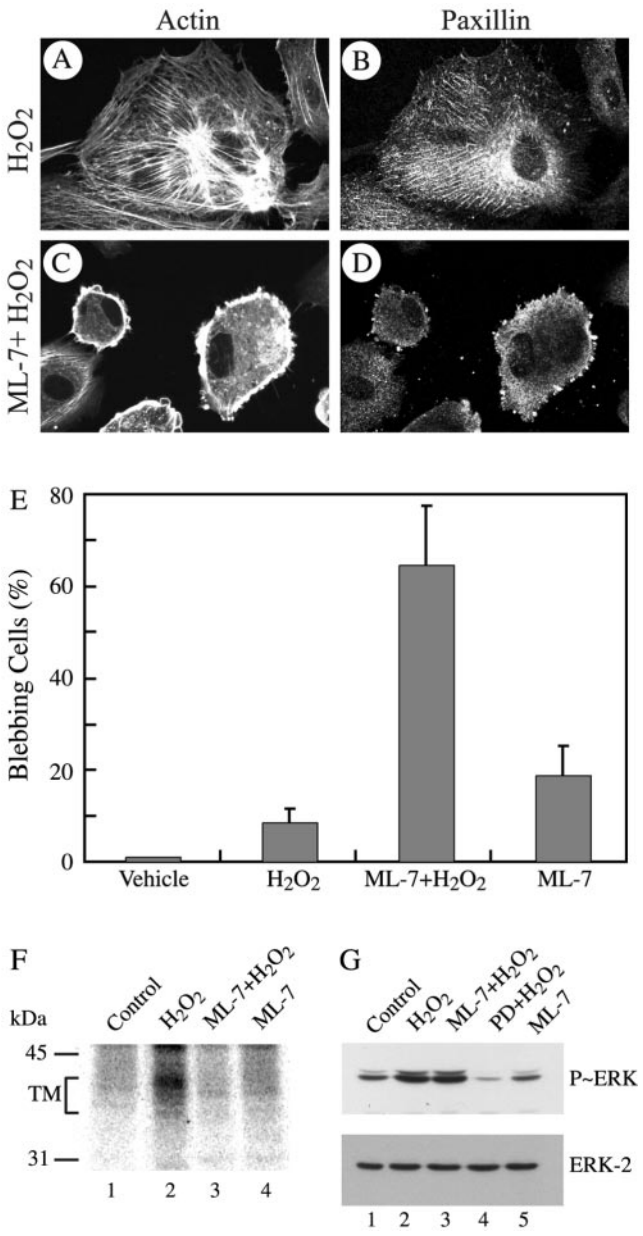


**Figure 9.** Inhibition of cellular contractility with ML-7 induces early membrane blebbing. Exponentially growing HUVECs were pretreated with vehicle (0.25% DMSO, 60 min; A and B) or with MLCK inhibitor ML-7 (25 $\mu$M, 60 min; C and D) and treated with 250 $\mu$M $H_2O_2$ for 5 min (A–D). After treatments, cells were fixed, permeabilized and stained for F-actin and paxillin as in Figure 3. In E, exponentially growing HUVECs were pretreated with vehicle (0.25% DMSO, 60 min) or with MLCK inhibitor ML-7 (25 $\mu$M, 60 min) and treated or not with 250 $\mu$M $H_2O_2$ for 30 min. After treatments, cells were processed as in A–D. Blebbing cells were counted, as in Figure 1, and mean from three separate experiments was calculated. (F) Exponentially growing HUVECs were labeled with $H_3[^{32}P]O_4$ and were pretreated simultaneously with the phosphatase inhibitor NaF (1 mM) and with vehicle (0.25% DMSO, 60 min; lanes 1 and 2), or with ML-7 (25 $\mu$M, 60 min; lanes 3 and 4) before being treated or not (lanes 1 and 4) for 30 min with 250 $\mu$M $H_2O_2$ (lanes 2 and 3). Proteins were extracted, immunoprecipitated using anti-tropomyosin antibody, and antigen–antibody complexes were run into 8.5% SDS-PAGE. Representative autoradiogram from two separate experiments is shown. (G) Exponentially growing HUVECs were pretreated with vehicle (0.25% DMSO, 60 min; lanes 1 and 2), or with ML-7 (25 $\mu$M, 60 min; lanes 3 and 5), or with PD098059 (50 $\mu$M, 60 min; lane 4) before being treated or not (lanes 1 and 5) for 5 min with 250 $\mu$M $H_2O_2$ (lanes 2, 3, and 4). Proteins were extracted, were run into 10% SDS-PAGE, and transferred on nitrocellulose membrane. Immunodectections with mouse monoclonal anti-phospho-ERK antibody (top) and rabbit polyclonal anti-ERK antibody (bottom) are shown.

Coleman *et al.*, 2001; Sebbagh *et al.*, 2001). In these cells, it is possible that caspase activation also led to a concomitant breakdown of focal adhesions and that the contractility generated through the RhoA pathway, instead of giving rise to the remodeling of actin into stress fibers, leads to membrane blebbing. We thus propose that the weakening of the membrane-actin and actin-substratum linkage that results from a defective assembly of focal adhesions due to unphosphorylation of tropomyosin combined with increased actin polymerization activity generated by SAPK2/p38, may all contribute to formation of blebs during exposure to $H_2O_2$ when ERK is blocked. When ERK was blocked, permanent damage to the endothelium was observed that was associated with a twofold increase in endothelial permeability to albumin. This likely results from the induced membrane blebbing that alters the interendothelial contacts. These findings strongly suggest that deregulation of the ERK–tropomyosin pathway in the presence of oxidative stress might be an underlying cause of endothelial dysfunction and thereby of diseases such as atherosclerosis that are associated with the incapacity of the endothelial cells to adequately cope with oxidants. In addition, the same phenomenon could contribute to increase microvascular permeability and contribute to end-organ damage in hypertension and other cardiovascular diseases (Plante *et al.*, 1996).

In summary, we have shown in this study that tropomyosin-1 is phosphorylated downstream of the ERK pathway in endothelial cells activated by oxidative stress. Inhibition of the ERK–tropomyosin pathway by PD098059 or a dominant negative form of ERK impaired the formation of focal adhesions and reduced the capacity of endothelial cells to resist oxidative stress. This was evidenced by the induction of intense membrane blebbing and breakdown of the endothelial layer. We conclude that the ERK-tropomyosin pathway is an essential determinant of the homeostatic response and cytoskeletal remodeling of endothelial cells to oxidative stress.

## ACKNOWLEDGMENTS

We thank Dr. Jacques Landry for providing anti-Myc tag (9E10) and anti-HA tag (12Ca5) mouse antibodies and Dr. Jean Charron for providing the anti-MEK1 #9 antibody. We thank Dr. Sylvain Meloche for providing pcDNANeo-HAP-MAPK plasmid and Dr. Jacques Pouysségur for providing pcDNANeo-MapkT192A and pECE-HA-MAPKK plasmids. We thank Dr. Claude Gravel for providing adenoviral vectors carrying $\beta$-galactosidase. We thank Dr. François Marceau and the Department of Obstetrics

(l'Hôpital St-François d'Assise) for providing umbilical cords. We also thank André Lévesque for help with microscopy. The work was supported the Canadian Institutes of Health Research grant MT15402 (to J.H.) S.R. holds a Postdoctoral Fellowship from the Canadian Institutes of Health Research, and M.L. holds an M.D./M.Sc. studentship from Le Fonds de Recherche en Santé du Québec.

## REFERENCES

Amano, M., Ito, M., Kimura, K., Fukata, Y., Chihara, K., Nakano, T., Matsuura, Y., and Kaibuchi, K. (1996). Phosphorylation and activation of myosin by Rho-associated kinase (Rho-kinase). J. Biol. Chem. *271*, 20246–20249.

Becker, L.C., and Ambrosio, G. (1987). Myocardial consequences of reperfusion. Prog. Cardiovasc. Dis. *30*, 23–44.

Chrzanowska-Wodnicka, M., and Burridge, K. (1996). Rho-stimulated contractility drives the formation of stress fibers and focal adhesions. J. Cell Biol. *133*, 1403–1415.

Coleman, M.L., Sahai, E.A., Yeo, M., Bosch, M., Dewar, A., and Olson, M.F. (2001). Membrane blebbing during apoptosis results from caspase-mediated activation of ROCK I. Nat. Cell Biol. *3*, 339–345.

Cooper, J.A. (2002). Actin dynamics: tropomyosin provides stability. Curr. Biol. *12*, R523–R525.

deBelle, I., and Mak, A.S. (1987). Isolation and characterization of tropomyosin kinase from chicken embryo. Biochim. Biophys. Acta *925*, 17–26.

Deschesnes, R.G., Huot, J., Valerie, K., and Landry, J. (2001). Involvement of p38 in apoptosis-associated membrane blebbing and nuclear condensation. Mol. Biol. Cell *12*, 1569–1582.

Finchman, V.J., James, M., Frame, M.C., and Winder, S.J. (2000). Active ERK/MAP kinase is targeted to newly forming cell-matrix adhesions by integrin engagement, and v-Src. EMBO J. *19*, 2911–2923.

Fischer, R.S., Lee, A., and Fowler, V.M. (2000). Tropomodulin and tropomyosin mediate lens cell actin cytoskeleton reorganization in vitro. Invest. Ophthalmol. Vis. Sci. *41*, 166–174.

Geiger, B., Bershadsky, A., Pankov, R., and Yamada, K.M. (2001). Transmembrane crosstalk between the extracellular matrix–cytoskeleton crosstalk. Nat. Rev. Mol. Cell. Biol. *2*, 793–805.

Gores, G.J., Herman, B., and Lemasters, J.J. (1990). Plasma membrane bleb formation and rupture: a common feature of hepatocellular injury. Hepatology *11*, 690–698.

Gunning, P., Hardeman, E., Jeffrey, P., and Weinberger, R. (1998). Creating intracellular structural domains: spatial segregation of actin and tropomyosin isoforms in neurons. Bioessays *20*, 892–900.

Heeley, D.H., Watson, M.H., Mak, A.S., Dubord, P., and Smillie, L.B. (1989). Effect of phosphorylation on the interaction and functional properties of rabbit striated muscle alpha alpha-tropomyosin. J. Biol. Chem. *264*, 2424–2430.

Huot, J., Houle, F., Marceau, F., and Landry, J. (1997). Oxidative stress-induced actin reorganization mediated by the p38 mitogen-activated protein kinase/heat shock protein 27 pathway in vascular endothelial cells. Circ. Res. *80*, 383–392.

Huot, J., Houle, F., Rousseau, S., Deschesnes, R.G., Shah, G.M., and Landry, J. (1998). SAPK2/p38-dependent F-actin reorganization regulates early membrane blebbing during stress-induced apoptosis. J. Cell Biol. *143*, 1361–1373.

Ishikawa, R., Yamashiro, S., and Matsumura, F. (1989). Differential modulation of actin-severing activity of gelsolin by multiple isoforms of cultured rat cell tropomyosin. Potentiation of protective ability of tropomyosins by 83-kDa nonmuscle caldesmon. J. Biol. Chem. *264*, 7490–7497.

Jacobs, D., Glossip, D., Xing, H., Muslin, A.J., and Kornfeld, K. (1999). Multiple docking sites on substrate proteins form a modular system that mediates recognition by ERK MAP kinase. Genes Dev. *13*, 163–175.

Kanthou, C., and Tozer, G.M. (2002). The tumor vascular targeting agent combretastatin A-4-phosphate induces reorganization of the actin cytoskeleton and early membrane blebbing in human endothelial cells. Blood *99*, 2060–2069.

Klemke, R.L., Cai, S., Giannini, A.L., Gallagher, P.J., de Lanerolle, P., and Cheresh, D.A. (1997). Regulation of cell motility by mitogen-activated protein kinase. J. Cell Biol. *137*, 481–492.

Lavoie, J.N., Champagne, C., Gingras, M.C., and Robert, A. (2000). Adenovirus E4 open reading frame 4-induced apoptosis involves dysregulation of Src family kinases. J. Cell Biol. *150*, 1037–1056.

Lee, A., Fischer, R.S., and Fowler, V.M. (2000). Stabilization and remodeling of the membrane skeleton during lens fiber cell differentiation and maturation. Dev. Dyn. *217*, 257–270.

Lees-Miller, J.P., and Helfman, D.M. (1991). The molecular basis for tropomyosin isoform diversity. Bioessays *13*, 429–437.

Leverrier, Y., and Ridley, A.J. (2001). Apoptosis: caspases orchestrate the ROCK 'n' bleb. Nat. Cell Biol. *3*, E91–E93.

Liu, H.P., and Bretscher, A. (1989). Disruption of the single tropomyosin gene in yeast results in the disappearance of actin cables from the cytoskeleton. Cell *57*, 233–242.

McCarthy, N.J., Whyte, M.K., Gilbert, C.S., and Evan, G.I. (1997). Inhibition of Ced-3/ICE-related proteases does not prevent cell death induced by oncogenes, DNA damage, or the Bcl-2 homologue Bak. J. Cell Biol. *136*, 215–227.

Miyazaki T., *et al*. (2000). Reciprocal role of ERK and NF-κB pathway in survival and activation of osteoclasts. J. Cell Biol. *148*, 333–342.

Mills, J.C., Stone, N.L., Erhardt, J., and Pittman, R.N. (1998). Apoptotic membrane blebbing is regulated by myosin light chain phosphorylation. J. Cell Biol. *140*, 627–636.

Mills, J.C., Stone, N.L., and Pittman, R.N. (1999). Extranuclear apoptosis. The role of the cytoplasm in the execution phase. J. Cell Biol. *146*, 703–708.

Miyoshi, H., Umeshita, K., Sakon, M., Imajoh-Ohmi, S., Fujitani, K., Gotoh, M., Oiki, E., Kambayashi, J., and Monden, M. (1996). Calpain activation in plasma membrane bleb formation during tert-butyl hydroperoxide-induced rat hepatocyte injury. Gastroenterology *110*, 1897–1904.

Nguyen, D.H., Catling, A.D., Webb, D.J., Sankovic, M., Walker, L.A., Somlyo, A.V., Weber, M.J., and Gonias, S.L. (1999). Myosin light chain functions downstream of Ras/ERK to promote migration of urokinase-type plasminogen activator-stimulated cells in an integrin-selective manner. 1999. J. Cell Biol. *146*, 149–164.

Pages, G., Lenormand, P., L'Allemain, G., Chambard, J.C., Meloche, S., and Pouyssegur, J. (1993). Mitogen-activated protein kinases p42mapk and p44mapk are required for fibroblast proliferation. Proc. Natl. Acad. Sci. USA *90*, 8319–8323.

Patton, W.F., Yoon, M.U., Alexander, J.S., Chung-Welch, N., Hechtman, H.B., and Shepro, D. (1990). Expression of simple epithelial cytokeratins in bovine pulmonary microvascular endothelial cells. J. Cell Physiol. *143*, 140–149.

Pelham, R.J. Jr., Lin, J.J., and Wang, Y.L. (1996). A high molecular mass non-muscle tropomyosin isoform stimulates retrograde organelle transport. J. Cell Sci. *109*, 981–989.

Phelps, P.C., Smith, M.W., and Trump, B.F. (1989). Cytosolic ionized calcium and bleb formation after acute cell injury of cultured rabbit renal tubule cells. Lab. Invest. *60*, 630–642.

Plante, G.E., Chakir, M., Ettaouil, K., Lehoux, S., and Sirois, P. (1996). Consequences of alteration in capillary permeability. Can. J. Physiol. Pharmacol. *74*, 824–33.

Ridley, A.J. (1999). Stress fibers take shape. Nat. Cell Biol. *1*, E64–E66.

Ridley, A.J., and Hall, A. (1992). The small GTP-binding protein rho regulates the assembly of focal adhesions and actin stress fibers in response to growth factors. Cell *70*, 389–399.

Riveline, D., Zamir, E., Balaban, N.Q., Schwarz, U.S., Ishizaki, T., Narumiya, S., Kam, Z., Geiger, B., and Bershadsky, A.D. (2001). Focal contacts as mechanosensors: externally applied local mechanical force induces growth of focal contacts by an mDia1-dependent and ROCK-independent mechanism. J. Cell Biol. *153*, 1175–1185.

Sano, K., Maeda, K., Oda, T., and Maeda, Y. (2000). The effect of single residue substitutions of serine-283 on the strength of head-to-tail interaction and actin binding properties of rabbit skeletal muscle alpha-tropomyosin. J. Biochem. *127*, 1095–1102.

Sastry, S.K., and Burridge, K. (2000). Focal adhesions: a nexus for intracellular signaling and cytoskeletal dynamics. Exp. Cell Res. *261*, 25–36.

Sebbagh, M., Renvoize, C., Hamelin, J., Riche, N., Bertoglio, J., and Breard, J. (2001). Caspase-3-mediated cleavage of ROCK I induces MLC phosphorylation and apoptotic membrane blebbing. Nat. Cell Biol. *3*, 346–352.

Sen, A., Chen, Y.D., Yan, B., and Chalovich, J.M. (2001). Caldesmon reduces the apparent rate of binding of myosin S1 to actin-tropomyosin. Biochemistry *40*, 5757–5764.

Shah, V., Bharadwaj, S., Kaibuchi, K., and Prasad, G.L. (2001). Cytoskeletal organization in tropomyosin-mediated reversion of ras-transformation: evidence for Rho kinase pathway. Oncogene *20*, 2112–2121.

Turner, C.E. (2000). Paxillin and focal adhesion signaling. Nat. Cell Biol. *2*, E231–E236.

Wang, P., Verin, A.D., Birukova, A., Gilbert-McClain, L.I., Jacobs, K., and Garcia, J.G.N. (2001). Mechanisms of sodium fluoride-induced endothelial cell barrier dysfunction: role of MLC phosphorylation. Am. J. Physiol. Lung Cell. Mol. Physiol. *281*, L1472–L1483.

Warren, K.S., Lin, J.L., McDermott, J.P., and Lin, J.J. (1995). Forced expression of chimeric human fibroblast tropomyosin mutants affects cytokinesis. J. Cell Biol. *129*, 697–708.

Watanabe, N., Kato, T., Fujita, A., Ishizaki, T., and Narumiya, S. (1999). Cooperation between mDia1 and ROCK in Rho-induced actin reorganization. Nat. Cell Biol. *1*, 136–143.

Watson, M.H., Taneja, A.K., Hodges, R.S., and Mak, A.S. (1988). Phosphorylation of $\alpha\alpha$- and $\beta\beta$-tropomyosin and synthetic peptide analogues. Biochemistry *27*, 4506–4512.

Wong, K., Wessels, D., Krob, S.L., Matveia, A.R., Lin, J.L., Soll, D.R., and Lin, J.J. (2000). Forced expression of a dominant-negative chimeric tropomyosin causes abnormal motile behavior during cell division. Cell Motil. Cytoskeleton *45*, 121–132.

Zhong, C., Chrzanowska-Wodnicka, M., Brown, J., Shaub, A., Belkin, A.M., and Burridge, K. (1998). Rho-mediated contractility exposes a cryptic site in fibronectin and induces fibronectin matrix assembly. J. Cell Biol. *141*, 539–551.